Supporting Information for:

Size-controlled large-diameter and few-walled carbon nanotube catalysts for oxygen reduction

Xianliang Wang,[a] Qing Li,[b] Hengyu Pan,[a] Ye Lin,[c] Yujie Ke,[a] Haiyang Sheng,[a] Mark T. Swihart*[a] and Gang Wu*[a]

[a] Department of Chemical and Biological Engineering, University at Buffalo (SUNY), Buffalo, New York 14260, USA

[b] Department of Chemistry, Brown University, Providence, Rhode Island 02912, USA

[c] Department of Chemical Engineering, University of South Carolina, Columbia, South Carolina 29208 , USA

Email: swihart@buffalo.edu (M.T.S); gangwu@buffalo.edu (G.W.)

(1) Diameter distributions of large-size carbon nanotubes produced using Fe, Co or Ni

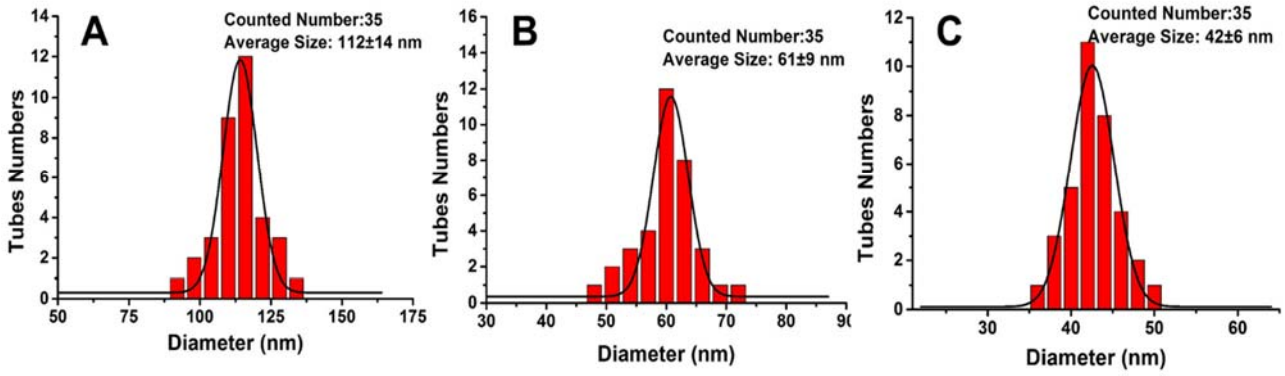

Figure S1. Diameter distributions of carbon nanotubes. The average diameter of the tubes are (A) Fe, 112 nm. (B) Co, 61 nm, (C) Ni, 42 nm.

(2) Typical Fe-derived carbon nanotube morphology

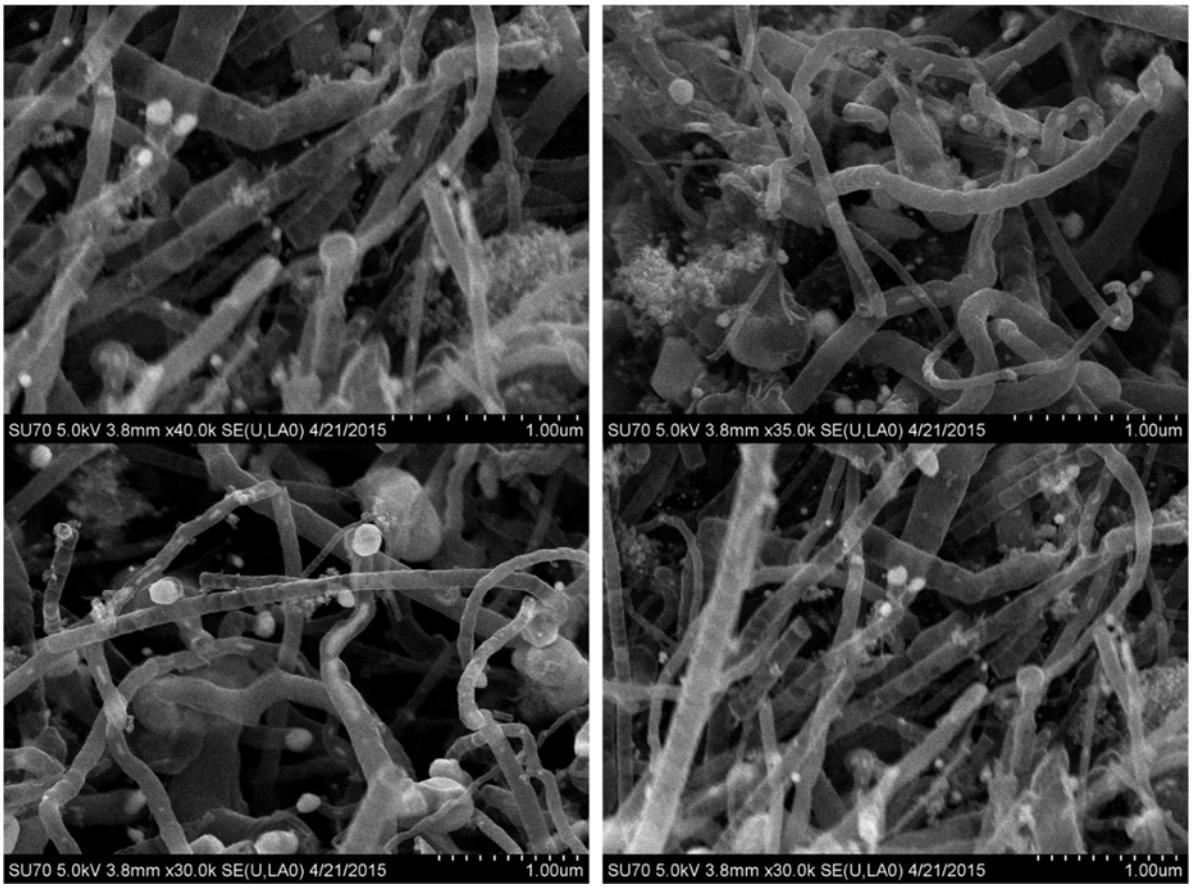

Figure S2. Representative SEM images of the largest Fe-derived carbon nanotubes prepared at 1000 ºC, showing uniform tube morphology.

(3) Effect of heating temperatures on carbon nanotube morphology.

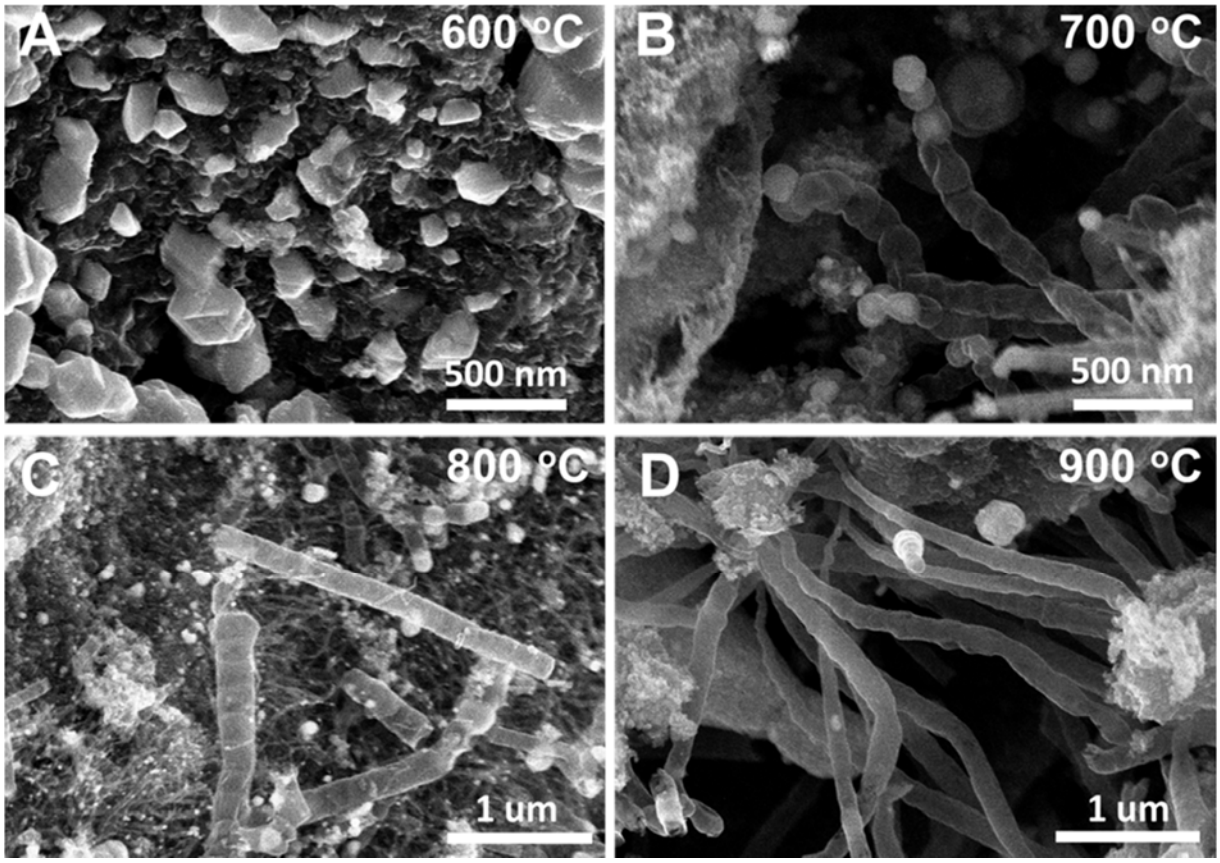

Figure S3. Representative SEM images of Fe-derived nitrogen doped carbon catalysts prepared at different temperatures: (A) 600 °C, (B) 700 °C, (C) 800 °C, and (D) 900 °C.

(4) Effect of heating temperatures on ORR activity

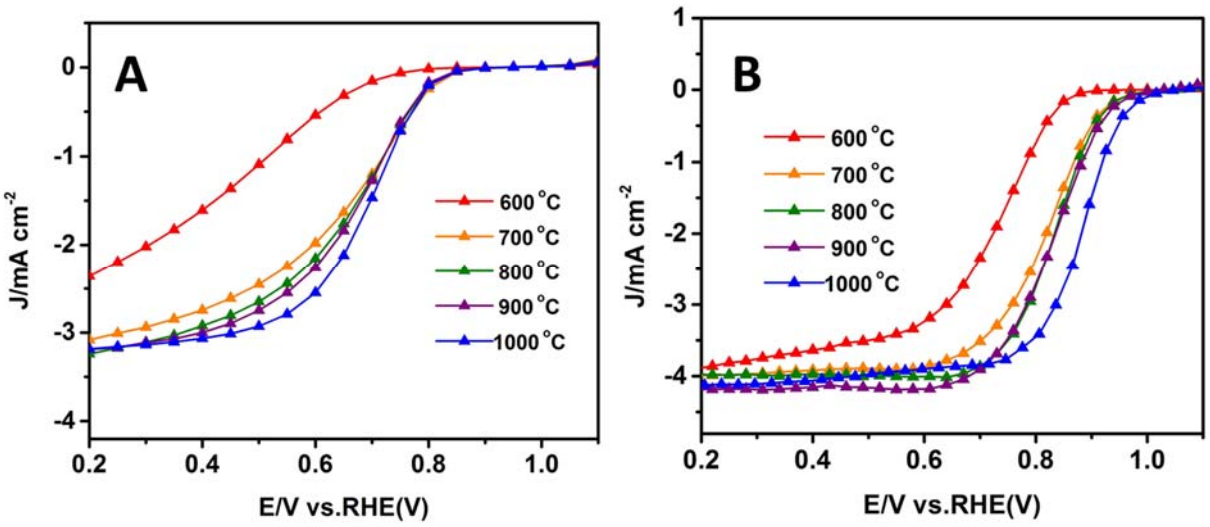

Figure S4. ORR steady-state polarization curves of Fe-derived samples as function of the 1st heating temperature ranging from 600 ºC to 1000 °C. Electrolytes: (A) 0.5 M H_2SO_4 and (B) 0.1 M NaOH.

(5) High-resolution XPS spectra of the C 1s

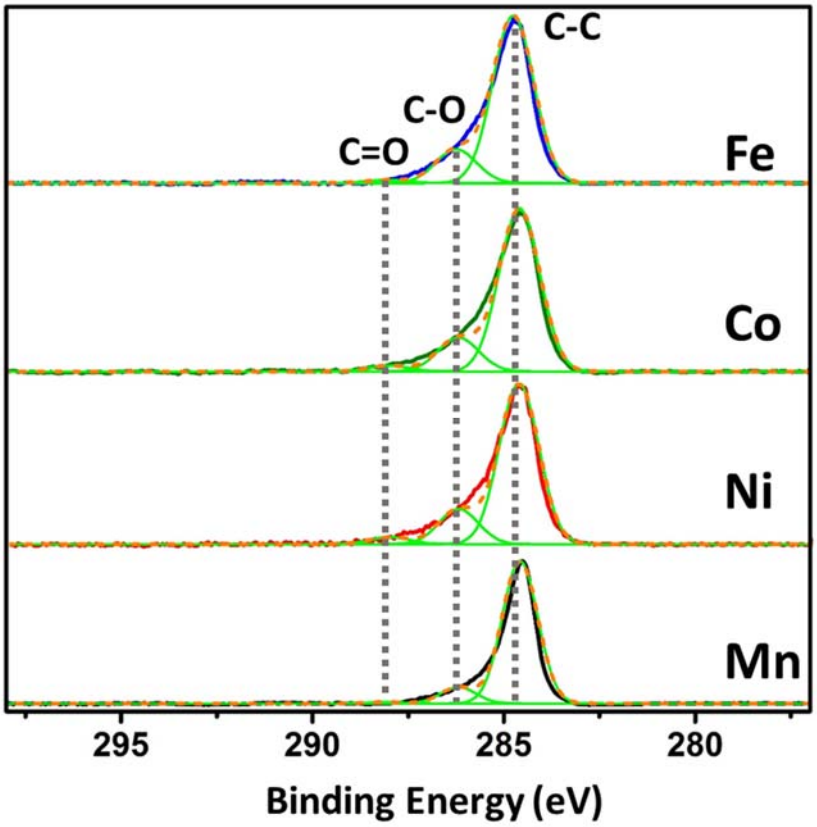

Figure S5. High-resolution XPS spectra of the C 1s region for the catalysts synthesized using Fe, Co, Ni or Mn. Spectra were deconvoluted into three peaks as labelled.

(6) BET surface area of carbon catalysts from various metals

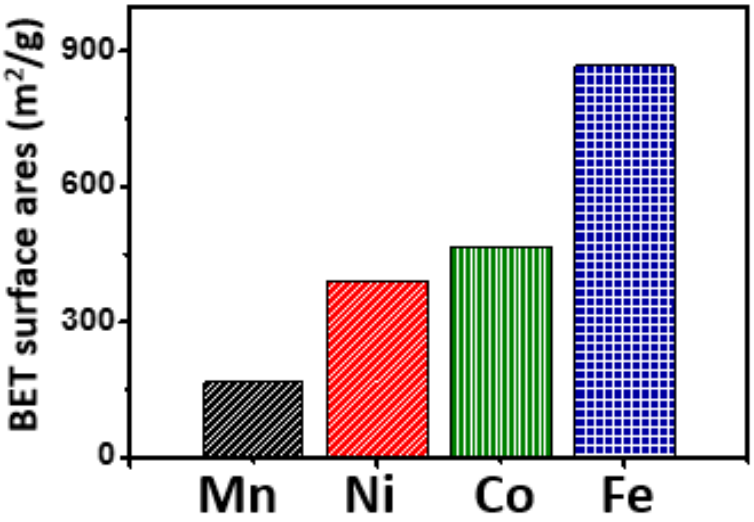

Figure S6. BET surface area of carbon catalysts as function of the metals used for the synthesis.

Table S1. Summary of BET and electrochemically accessible surface area of catalysts

Transition Metal	BET surface area m^2/g	S_a in acidic media		S_a in alkaline media	
		S_a m^2/g	S_a/BET	S_a m^2/g	S_a/BET
Fe	868	419	0.48	403	0.46
Co	466	328	0.70	294	0.63
Ni	391	256	0.65	241	0.62
Mn	167	144	0.86	122	0.73

(7) Nitrogen adsorption–desorption of Fe-derived N-CNTs, Co-derived N-CNTs, Ni-derived N-CNTs and Mn-derived N-CCs.

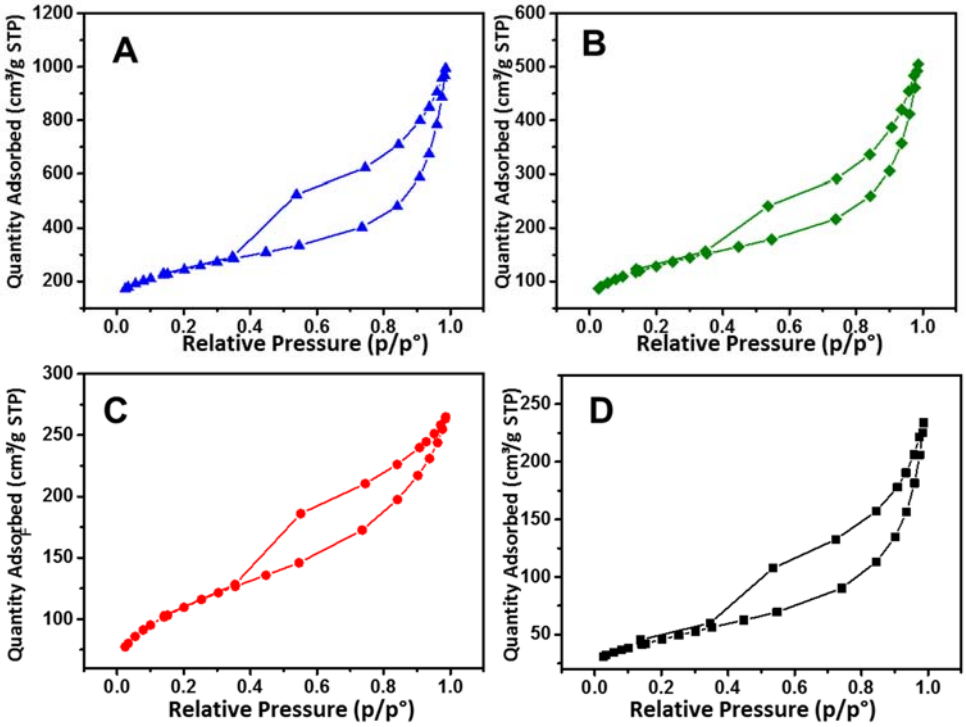

Figure S7. N_2 adsorption-desorption isotherms of Fe- (A), Co- (B), Ni- (C), and Mn-derived nitrogen-doped carbon catalysts (D) at 77 K.

(8) Steady-state polarization curves for Co- and Fe-derived catalysts before and after the second heat treatment

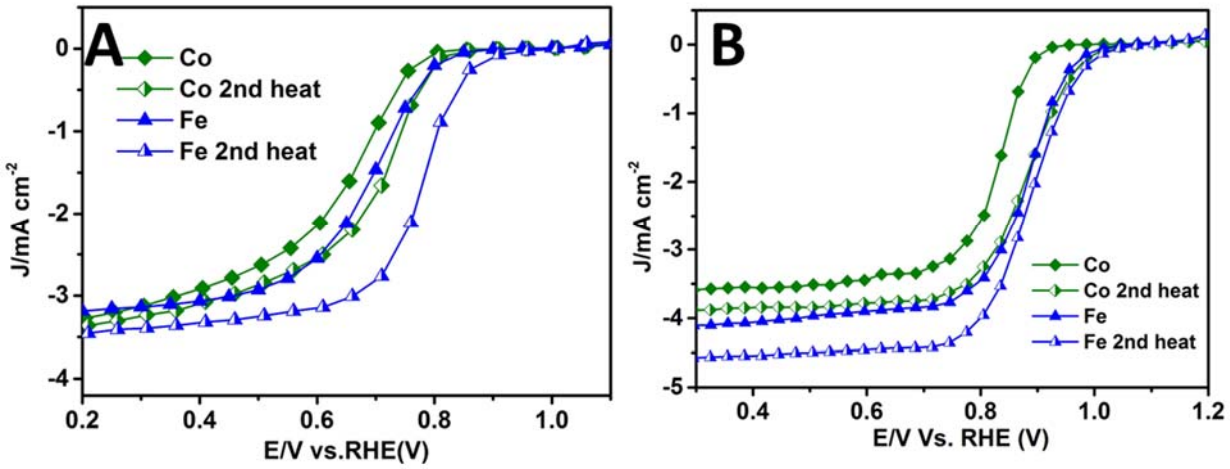

Figure S8. Steady-state ORR polarization plots for Fe and Co-derived catalysts before and after the second heat treatment. Electrolytes: (A) 0.5 M H_2SO_4 and (B) 0.1 M NaOH.

(9). XPS spectra of N 1s for Fe- and Co-derived catalysts before and after the second heat treatment.

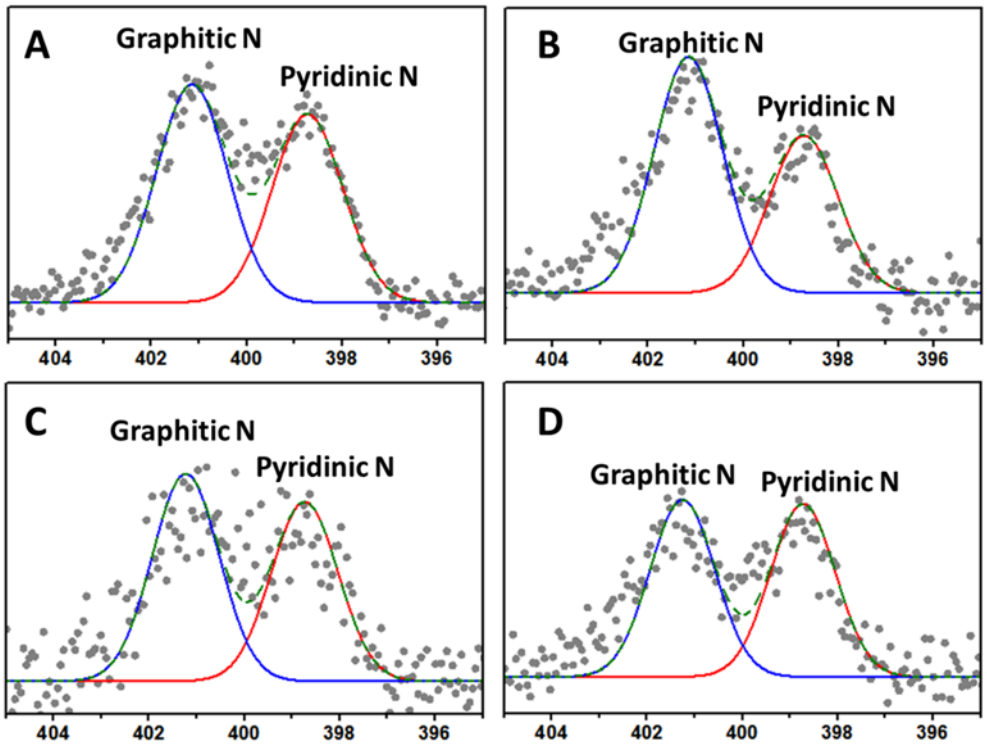

Figure S9. XPS spectra of N 1s for the carbon catalysts synthesized using Fe (A, B) and Co (C, D) before (A, C) and after (B, D) the second heat treatment.

Table S2 Summary of elemental composition of carbon catalysts derived from Fe or Co before and after the second heat treatment (* indicate the content after second heat treatment)

Catalysts	Atomic concentration, at%			
	M/M*	C/C*	O/O*	N/N*
Fe	0.43/0.56	90.39/94.98	4.69/1.53	4.49/2.93
Co	1.22/1.29	90.33/92.57	4.23/1.75	4.22/4.39

(10). XPS spectra of C 1s for Fe- and Co-derived N-CNTs before and after second heat treatment.

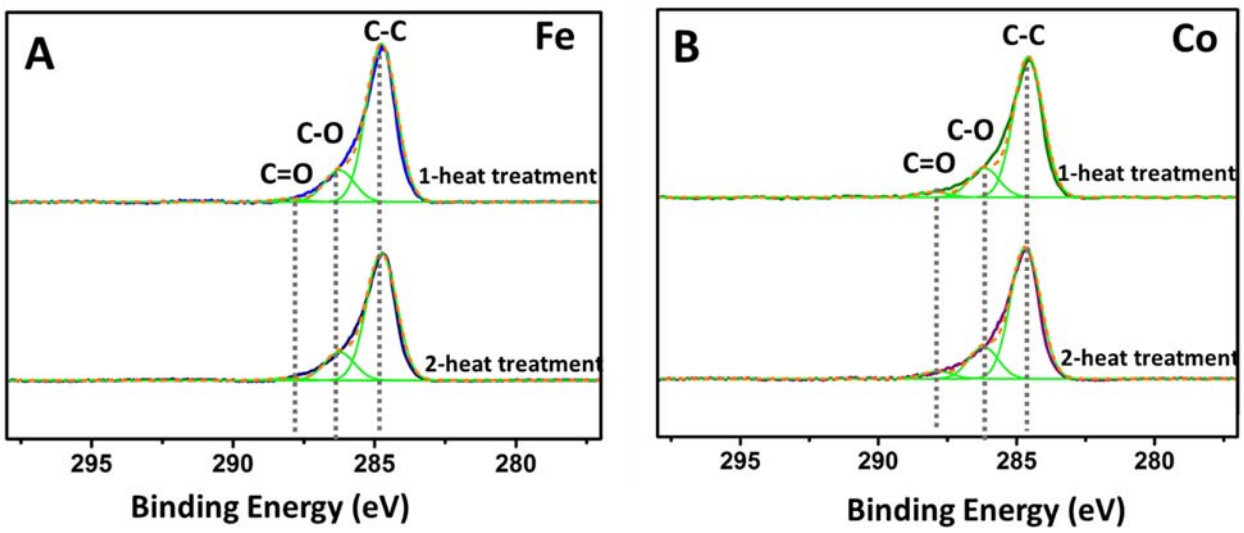

Figure S10. XPS spectra of C 1s for the samples synthesized using (A) Fe, and (B) Co before and after second heat treatment.